

**Generation of mice transgenic for human *CYP2C18* and *CYP2C19*.**

**Characterization of the sexually dimorphic gene- and enzyme expression.**

Susanne Löfgren\*, R. Michael Baldwin\*, Masahiro Hiratsuka, Annelie Lindqvist, Anne Carlberg, Sarah C Sim, Meint Schülke, Michael Snait, Anne Edenro, Ronny Fransson-Steen, Ylva Terelius and Magnus Ingelman-Sundberg

**Primary Laboratory of Origin**

Department of Physiology and Pharmacology, Section of Pharmacogenetics, Karolinska Institutet, SE-171 77 Stockholm, Sweden: RMB, MH, AC, SCS, MIS

Safety Assessment Sweden, AstraZeneca R&D Södertälje, SE-15185 Södertälje, Sweden: SL, RFS

Research DMPK, AstraZeneca R&D Södertälje, SE-15185 Södertälje, Sweden: AL, YT

AstraZeneca Transgenics & Comparative Genomics (ATCG), AstraZeneca R&D, Mölndal; SE-731 83 Mölndal, Sweden: MSc, AE

Cambridge Antibody Technology, Milstein Building Granta Park, Cambridge, CB21 6GH, United Kingdom: MSn

**Running title:** Transgenic CYP2C18/19 mice

**Corresponding Author**

R. Michael Baldwin

Section of Pharmacogenetics

Department of Physiology and Pharmacology

Karolinska Institutet

Nanna Svartz vag 2

SE-17177 Stockholm Sweden

+46 8 524 87711 (w)

+46 73 994 3277 (m)

+46 8 337327 (fax)

mike.baldwin@ki.se

Number of text pages: 38

Number of tables: 2

Number of figures: 7

Number of references: 37

Number of words Abstract: 250

Number of words Introduction: 456

Number of words Discussion: 1296

## **Abbreviations**

BAC, bacterial artificial chromosome

CAR, constitutive androgen receptor

DAPI, 4',6-diamidino-2-phenylindole

DMEM, Dulbecco's modified Eagle's medium

FBS, fetal bovine serum

FISH, fluorescent in situ hybridization

GAPDH, glyceraldehyde 3-phosphate dehydrogenase

gDNA, genomic DNA

GH, growth hormone

Het, heterozygous transgenic mouse

HPRT, hypoxanthine guanine phosphoribosyltransferase

HRP, horse radish peroxidase

PXR, pregnane X receptor

TBS, Tris-buffered saline

Tg, transgenic mouse

wt, wildtype

## Abstract

CYP2C19 is an important enzyme for human drug metabolism, and it also participates in the metabolism of endogenous substrates, whereas the CYP2C18 enzyme is not expressed in human liver despite high mRNA expression. Mice transgenic for the human *CYP2C18* and *CYP2C19* genes were generated. Quantitative mRNA analysis showed CYP2C18 and CYP2C19 transcripts in liver, kidneys and heart to be expressed in a sexually dimorphic manner, with male mice having 2- to 100-fold higher levels. Transcript levels in the small intestine were somewhat higher than liver, but were similar in both sexes. Transgene mRNA expression was much lower in lung and brain and least in the heart. Immunoblotting using an antipeptide antiserum, reactive with human CYP2Cs and mouse CYP2C70, revealed increased immunoreactive protein in liver microsomes from heterozygous transgenic male mice and a concomitant increase in 5'-hydroxylation of *R*-omeprazole and *S*-mephenytoin intrinsic clearance, consistent with CYP2C19 overexpression. A CYP2C18 specific antiserum showed that this enzyme was not expressed in livers or kidneys from heterozygous transgenic mice, but the antiserum had high affinity for recombinant CYP2C18 expressed in COS-7 cells. It is concluded that i) both the *CYP2C18* and *CYP2C19* genes are subject to sexually dimorphic regulation in murine liver, kidney and heart, ii) the CYP2C18 protein is not expressed in murine liver or kidney despite high levels of the corresponding mRNA, and iii) this transgenic model might be suitable for studying sex dependent regulation of the human *CYP2C* genes and possibly serve as an *in vivo* model for CYP2C19-dependent drug metabolism.

## Introduction

Cytochrome P450 2C (CYP2C) enzymes are heme-containing monooxygenases responsible for the metabolism of many endogenous and xenobiotic compounds. In humans, the CYP2C subfamily contains four members, CYP2C8, CYP2C9, CYP2C18 and CYP2C19, which together are involved in the metabolism of approximately 20% of clinically used drugs (Goldstein, 2001). In addition to exogenous substrates, CYP2C enzymes metabolize arachidonic acid and some steroids (Nebert and Russell, 2002), and the action of CYP2C9 has been implicated in the regulation of vascular tone (Hillig et al., 2003).

Each member of the human CYP2C subfamily has been shown to be genetically polymorphic. Polymorphisms within the *CYP2C19* gene have been shown to affect the metabolism of many commonly used drugs such as the anticonvulsant mephenytoin, proton pump inhibitors such as omeprazole, the anxiolytic agent diazepam, certain antidepressants, and the antimalarial drug proguanil (Ingelman-Sundberg et al., 2007). The success rate of treatment with omeprazole has been highly correlated with *CYP2C19* genotype (Furuta et al., 1998; Klotz, 2006).

Natural and synthetic glucocorticoids (agonists and antagonists), as well as other clinically important drugs, induce the hepatic CYP2B, CYP2C and CYP3A subfamilies in man. Induction can lead to clinically important drug-drug interactions (Pascucci et al., 2003). The constitutive androgen receptor (CAR) and pregnane X receptor (PXR) are known to be involved in the regulation of *CYP2C19*, suggesting a constitutive regulation by endogenous hormones as well as by drugs such as rifampicin and dexamethasone (Gerbal-Chaloin et al., 2001; Chen et al., 2003). Drug-drug interactions,

together with genetic polymorphisms in CYP2C enzymes, greatly contribute to the variation in oral bioavailability and systemic clearance of CYP2C substrates. This variation is particularly undesirable for drugs with narrow therapeutic indices.

The 4'-hydroxylation of *S*-mephenytoin is a well established *in vitro* and *in vivo* metric of CYP2C19 enzymatic activity (Meier et al., 1985; Walsky and Obach, 2004).

*S*-mephenytoin 4'-hydroxylation has been shown to take place at a higher rate in human liver microsomes than in microsomes from mice (Bogaards et al., 2000).

*S*-mephenytoin metabolism, measured as *S*-mephenytoin disappearance, has been shown to be similar between male and female mice of five commonly used laboratory strains (Lofgren et al., 2004). Furthermore, the 5'-hydroxylation of omeprazole is a similarly well established marker for CYP2C19 activity (Niioka et al., 2007).

To obtain a better *in vivo* model system to study the role of human CYP2C enzymes in drug pharmacology and toxicology and to investigate the transcriptional regulation of these genes, we have generated a gene-addition transgenic mouse containing the human *CYP2C18* and *CYP2C19* genes. We find that both human *CYP2C* genes are subject to tissue-specific sexually dimorphic transcriptional regulation. Furthermore, the *CYP2C19* gene, but not the *CYP2C18* gene, is expressed in the mouse liver to yield a catalytically active enzyme as indicated by *S*-mephenytoin and *R*-omeprazole metabolism.

## Materials and Methods

### *Chemicals and antibodies*

Oligonucleotide PCR primers were purchased from Invitrogen (Paisley, Scotland). Bovine serum albumin and  $\beta$ -NADPH were obtained from Sigma Chemicals Co. (St Louis, MO). *S*-mephenytoin and the reference (+/-)-4'-hydroxy mephenytoin were purchased from Toronto Research Chemicals (North York, ON, Canada). *R*-Omeprazole and internal standard (H 259/36, AstraZeneca) were kind gifts from Dr Leif Bertilsson, Karolinska Institutet, Stockholm, Sweden. 5'-hydroxyomeprazole was supplied by AstraZeneca (Möln dal, Sweden). An antiserum specific against CYP2C18 was kindly donated by Dr. Eric Johnson, The Scripps Research Institute, La Jolla, California, USA (Richardson et al., 1997). An antipeptide antiserum ( $\alpha$ -hCYP2C), targeted against the four C-terminal amino acids of the four human CYP2Cs and coincidentally mouse CYP2C70, was kindly donated by Dr. Robert Edwards, Section of Experimental Medicine and Toxicology, Imperial College, London, UK (Edwards et al., 1998). In liver microsomes from transgenic mice this antiserum is expected to react only with CYP2C70, CYP2C18 (if present) and CYP2C19, whereas in human liver microsomes the serum will react also with CYP2C8 and CYP2C9. Recombinant CYP2C18 standard (Supersomes<sup>TM</sup>) was purchased from BD Biosciences (San Jose, CA). All other chemicals and reagents were of analytical grade from commercial sources.

### *Animals and generation of transgenic CYP2C18/19 mice*

Transgenic mice containing the human *CYP2C18* and *CYP2C19* genes were generated from human BAC clone RP11-466J14, which was reported to contain both complete *CYP2C18* and *CYP2C19* genes. The BAC clone was confirmed by both restriction

digestion and sequencing of the 5' and 3' ends, revealing the 5' end to begin 5828 bases upstream from the start of *CYP2C18* exon 1 (RefSeq: NM\_000772) and the 3' end to contain an additional 30,869 bases downstream from the end of *CYP2C19* exon 9 (RefSeq: NM\_000769) (Figure 1). BAC DNA was isolated (Midi Prep, Qiagen, Valencia, CA) and digested with the restriction enzyme *NotI* to release the insert which was then isolated on a Sepharose gel column. Purified BAC DNA was injected into C57BL/6 eggs and founders were identified by genotyping of genomic DNA extracted from tail biopsies (described below). The subsequent transgenic CYP2C18/19 mice were reared and studied at several locations: AstraZeneca Transgenic Centre (Mölndal, Sweden), AstraZeneca Bioscience (Södertälje, Sweden) and Karolinska Institutet (Stockholm, Sweden). All transgenic CYP2C18/19 mice, with the exception of the nine-week old mice used as one group in the *S*-mephenytoin microsomal metabolism studies, were offspring from a transgenic CYP2C18/19 mouse and wildtype (wt) breeding, and thus, were heterozygous for the transgene. A small number of the transgenic nine-week old mice used in the *S*-mephenytoin studies were heterozygous offspring from crossing two transgenic mice.

#### *PCR Genotyping*

To identify mice possessing the CYP2C18/19 transgene, genomic DNA (gDNA) was extracted from tail or ear tissue using either established protocols (Sambrook and Russell, 2001) or a commercial kit (DNeasy Tissue, Qiagen). Amplification of gDNA was performed in a 20  $\mu$ l reaction volume containing 10  $\mu$ l HiFi PCR MasterMix (ABgene House, Surrey, UK), 250 nM of each primer and 1  $\mu$ l gDNA. The four different gene specific primer pairs are listed in Table 1. The PCR thermoprofile consisted of initial denaturation for 2 min at 94  $^{\circ}$ C, followed by 30 cycles of 10 s at



94 °C, 20 s at 60 °C and 45 s at 68 °C, followed by a 3 min extension at 70 °C.

Amplification products were visualized with ethidium bromide/agarose gel electrophoresis.

#### *Total RNA isolation and cDNA synthesis for real time PCR*

Transgenic and wt control mice were killed via carbon dioxide inhalation. Whole livers, kidneys, heart, lung, brain, and 2-3 cm sections of proximal small intestine (~duodenum) from 26-31 week old male and female mice were placed in RNAlater (Qiagen) according to the manufacturer's recommendations. At the same time, sections of either ear or tail were removed for genomic DNA isolation and genotyping (described above). Total RNA was extracted from approximately 10 milligrams of tissue using a commercially available kit (RNeasy, Qiagen). DNA was removed with DNase digestion (Qiagen). The quality of extracted RNA was assessed by UV spectrophotometry and direct visualization via formaldehyde-agarose gel electrophoresis. RNA was reverse-transcribed into first strand cDNA using 0.5 µg total RNA, 4 µl 5x reaction buffer, 5 µM Oligo (dT)<sub>18</sub>, 0.5 mM dNTPs, 10mM DTT, 1 µl RNaseOut (Invitrogen, Carlsbad, CA), and 200 U of Superscript II RNase H- reverse transcriptase (Invitrogen) in a 20 µl reaction volume. Reactions were incubated at 42 °C for 60 min followed by inactivation at 70 °C for 10 min. To address the possibility of genomic DNA contamination, reverse transcription reactions were also run in the absence of reverse transcriptase.

#### *Primers design for real time PCR*

The primer pairs for the amplification of CYP2C19 and CYP2C18 transcripts were targeted to sequences showing relatively low homology with the endogenous murine

CYP2C isoforms using a multiple sequence alignment (ClustalW). Multiple potential primers for real-time PCR were evaluated with the following criteria; observation of a single melting curve peak, visualization of a single amplicon of the appropriate length following agarose gel electrophoresis, direct sequencing of amplicons, amplification efficiencies >95%, and the absence of amplification products using either liver cDNA derived from wt mice or reverse transcriptase minus controls. Ultimately, the best CYP2C19 primer pair was obtained by minor modification of those used previously by Klose et al. (Klose et al., 1999). Murine hypoxanthine guanine phosphoribosyltransferase (HPRT) and glyceraldehyde 3-phosphate dehydrogenase (GAPDH) were used as normalization factors. Primer sequences are shown in Table 1.

#### *Real time quantitative PCR*

To quantitate the expression of CYP2C18 and CYP2C19 transcripts, reaction mixtures for real-time PCR were 25  $\mu$ l and contained the following: 12.5  $\mu$ l 2x SYBR Green Master Mix (Applied Biosystems, Foster City, CA), 0.25  $\mu$ l cDNA and the appropriate primer pair (400 nM). The PCR thermoprofile consisted of initial activation of the polymerase at 95 °C for 10 min followed by 40 PCR cycles of 95 °C for 20 s, 58 °C for 30 s and 72 °C for 30 s. Assays were performed in triplicate on an Applied Biosystems 7500 Fast Real-Time PCR system. Relative CYP2C transgene expression levels were determined using qBase version 1.3.5 (Hellemans et al., 2007). CYP2C18 and CYP2C19 expression levels were normalized using the geometric mean of HPRT and GAPDH according to established methodologies (Vandesompele et al., 2002).

#### *FISH analysis*

Two heterozygous mice were crossed and primary mouse embryonic fibroblasts were obtained and cultured according to established methods. Four cell lines were established, two for heterozygous animals and two for homozygous animals. After five days of cell culture (DMEM, 10% FBS), chromosome preparations were made according to standard cytogenetic techniques. Approximately 30  $\mu$ l of the chromosome preparation was dropped onto a slide, air-dried and baked at 60 °C for one hour followed by DAPI staining for ~10 min.

Approximately 2  $\mu$ g DNA from two different preparations of linearized BAC clone insert were labelled with either 20mM biotin-dUTP or 20mM digoxigenin-dUTP by a standard nick translation procedure (90 min, 15°C). Probe length was analyzed on a 1% agarose gel. The probes showed the optimal average length of ~300 bp after nick translation. Approximately 50 ng DNA in 10  $\mu$ l hybridization buffer (50% formamide, 2x SSC, 10% dextran sulfate) was applied to chromosomes fixed on the slide, mounted with a cover slip and sealed with rubber cement. Probe DNA and chromosomes were denatured together at 72 °C for 3 min. Hybridization was overnight at 37 °C in a wet chamber. After hybridization, the cover slip was removed and the slide was washed in 2x SSC for 8 min. Slides were then incubated at 72 °C in 0.4x SSC/0.1% Tween 20 for 1 min. For probe detection, both an anti-digoxigenin antibody coupled with rhodamin and avidin coupled with FITC were incubated for 30 min at 37 °C in 4x SSC/0.1% Tween/5% BSA followed by two 10 min washes in 4x SSC/0.1% Tween. Slides were then stained in DAPI for 10 min. DAPI stained chromosomes and *in situ* hybridization signals were analyzed on a Zeiss Axioplan II microscope. For an optimal identification of chromosome banding, DAPI stained metaphases were imaged prior to probe hybridization. Each image field (blue, green and orange) was recorded separately with a

b/w CCD camera (SenSys, Photometrics). Chromosomes and FISH signals were then displayed in false colors and images merged with SmartCapture X software (Digital Scientific, Cambridge, UK).

#### *Gene copy number determination*

Transgene copy number was approximated using a real-time PCR approach based on existing methodologies (De Preter et al., 2002; Hoebeek et al., 2007). Briefly, the efficiency and specificity of primer pairs for *CYP2C19*, human *IL2* (*hIL2*) and mouse *IL2* (*mIL2*) genomic sequences were evaluated using serial two-fold dilutions of mouse and human genomic DNA (gDNA) ranging from 2 to 0.25 ng (primer sequences shown in Table 1). gDNA was quantified fluorometrically using PicoGreen (Invitrogen).

Reaction mixtures were 25  $\mu$ l and contained the following: 12.5  $\mu$ l 2 x SYBR Green Master Mix (Applied Biosystems), human or mouse gDNA and the appropriate primer pair (400 nM). The PCR thermoprofile consisted of initial activation of the polymerase at 95 °C for 10 min followed by 40 PCR cycles of 95 °C for 15 s, 60 °C for 1 min followed by a melting curve to verify the presence of a single amplification product. Assays were performed in triplicate on an Applied Biosystems 7500 Fast Real-Time PCR system. Subsequently, 1 ng of gDNA from four heterozygous mice and four humans were amplified using the same PCR conditions and the relative amounts of *CYP2C19* and *hIL2* were determined for each human gDNA sample along with *CYP2C19* and *mIL2* in each mouse gDNA sample. To calculate the mouse *CYP2C19* copy number relative to the human gDNA samples, the following equation was used: relative copy number difference =  $(1+E)^{-\Delta Ct_{2C19}} / (1+E)^{-\Delta Ct_{IL2}}$  (E=efficiency of the PCR reaction;  $\Delta Ct_{2C19}$  = difference in mean *CYP2C19* threshold cycle values between

mouse and human gDNA samples;  $\Delta\text{Ct IL2}$  = difference in mean IL2 threshold cycle values between mouse and human gDNA samples).

#### *Microsomal Preparation*

Microsomes were prepared from individual male and female mouse livers and kidneys according to standard methodologies (Maines, 1999). Briefly, tissues were homogenized in 15-20 ml buffer (10 mM sodium/potassium-phosphate/1.14% KCl, pH 7.4) at 0-4 °C followed by centrifugation (10,000 g, 10 min) and subsequent centrifugation of the supernatant (105,000 g for 90 min). Microsomal pellets were resuspended in 50 mM potassium phosphate buffer (0.4 ml per gram liver) and stored at -80 °C. Microsomal cytochrome P450 content was quantified spectrophotometrically using a CARY 400 UV-VIS spectrophotometer from the CO-difference spectra of dithionite-reduced samples using an extinction coefficient of  $91 \text{ mM}^{-1} \text{ cm}^{-1}$  between 450 and 490 nm (Omura and Sato, 1964). Protein was quantified using a scaled down version of the original method by Lowry et al. and bovine serum albumin was used as a standard (Lowry et al., 1951).

#### *S-Mephenytoin hydroxylation*

The metabolism of *S*-mephenytoin to its major CYP2C19-dependent metabolite 4'-hydroxy (4-OH) mephenytoin was studied using liver microsomes from nine-week old heterozygous transgenic and wt mice. The rates of mephenytoin 4'-hydroxylation were determined in incubations containing liver microsomes (100  $\mu\text{g}$  microsomal protein) and *S*-mephenytoin (10, 25, 50, 100 and 250  $\mu\text{M}$  from a stock solution in ethanol, giving a final ethanol concentration of 1% in each incubation) in a total volume of 200  $\mu\text{l}$  50 mM potassium phosphate buffer, pH 7.4. Reactions were incubated at

37 °C for 3-5 min prior to the addition of NADPH (1 mM final concentration) to initiate metabolism. Incubations were performed in duplicate for 0, 5, 10 and 20 min.

Additional incubations without NADPH or microsomal protein were used as negative controls. Reactions were terminated by the addition of one volume ice-cold acetonitrile. Precipitated proteins were removed by centrifugation (12,000 g, 10 min, 4 °C) followed by LC-MS/MS analysis of the supernatant.

Michaelis-Menten kinetics were assumed and apparent  $K_m$  and  $V_{max}$  were estimated for each animal using Lineweaver-Burke plots. Incubations containing *S*-mephenytoin at the two lowest concentrations (10 and 25  $\mu$ M) were excluded from analysis as the observed levels of the 4'-OH metabolite were below the limit of quantification in several instances. The apparent  $K_m$ ,  $V_{max}$  and  $Cl_{int}$  values from the majority of nine-week old mice could be calculated using both the total amount of microsomal protein and nmoles of total P450. In the 3 instances where hepatic microsomal protein yields were insufficient for the spectral quantification of P450 content, kinetic constants were instead determined solely on the basis of microsomal protein content.

#### *High-performance liquid chromatography and mass spectroscopy for detection of mephenytoin metabolism*

Chromatographic separations were performed using a three-column LC-system described previously (Lindqvist et al., 2004). Briefly, three High Purity 5  $\mu$ m, 50 x 2.1 mm i.d. columns were used with a binary gradient consisting of a mixture of acetonitrile: water: glacial acetic acid (2:98:0.1 and 80:20:0.1) at a flow rate of 0.4 ml/min. The injection volume was 20  $\mu$ l. Fractions were analyzed by MS/MS using electrospray ionisation with multiple reaction monitoring on a Quattro Micro

(Micromass UK Limited, Manchester, UK). The dwell time for each transition was 0.1 s. The desolvation and source temperature were 250 °C and 120 °C, respectively. The cone and desolvation gas flows were 130 L/h and 920 L/h, respectively. Nitrogen and argon were used as cone and collision gases, respectively. Transitions, mode, cone voltage and collision energy used for *S*-mephenytoin and its metabolite were 217.07>188.26, ESP, CV=30, CE=22 and 233.14>161.05, ESP, CV=28 CE=22, respectively.

#### *Analysis of omeprazole metabolism*

*R*-omeprazole was used as an additional probe drug for CYP2C19 activity in microsomes from male transgenic mice. The rate of 5'-hydroxy omeprazole generation was determined essentially as previously published (Tybring et al., 1997). Liver microsomes for *R*-omeprazole studies and Western blotting (described below) were prepared from 12-week old male wt mice or from age-matched transgenic male mice which had previously been control animals sham operated eight weeks before sacrifice and isolation of microsomes. The sham-operated mice were subjected to 30 minutes of general anesthesia and were utilized to minimize the total number of transgenic mice used in the present study. Prior to sample analysis, the linearity of metabolite formation versus both the amount of microsomal protein and incubation time were evaluated. The incubation mixture (200 µl) contained 50 µg protein, 10 µM *R*-omeprazole, 1 mM freshly made NADPH and 50 mM potassium phosphate buffer pH 7.4. Incubations were carried out for 15 min and were stopped with the addition of 800 µl dichloromethane:acetonitrile 9:1 and an internal standard (H 259/36, AstraZeneca). All samples were extracted for ten minutes using a vortex mixer followed by centrifugation (2000 g, 10 min) and aspiration of the plasma/aqueous phase. The organic phase was

transferred to a new tube and evaporated to dryness at 60 °C. Samples were reconstituted in 100 µl of 10 mM disodium phosphate buffer (pH 9.3). Chromatography was performed using a Varian Prostar R-HPLC system, consisting of a Model 240 solvent delivery module, Model 310 UV-Vis detector and a Model 410 autosampler, combined with a LiChrospher 60 RP-select B 125 mm x 4 mm, 5 µm particle, column and an identical 4 mm x 4 mm precolumn (Merck, Darmstadt, Germany). The mobile phases were 62.5 mM ammonium acetate pH 7.0 (A) and acetonitrile (B). The solvent gradient was as follows; initially 80% A:20% B with a linear ramp to 55% A:45% B from 2 min to 18 min, a linear return to initial condition from 23 min to 27 min followed by a 5 min equilibration prior to injection of the next sample. The flow rate was 1 ml/min. Metabolites and internal standard were monitored via absorbance at 302 nm and peak areas determined using the Varian Star version 5.51 software package.

#### *Expression of CYP2C18 in cultured cells*

A pCMV6-XL5 construct of CYP2C18 purchased from Origene (Rockville, MD) was transiently transfected into Huh-7 and COS-7 cells. In brief, cells were maintained at 37 °C in an atmosphere of 5% CO<sub>2</sub> in modified DMEM medium supplemented with FBS, sodium pyruvate, and antibiotics. For transfection experiments, cells (1.5 x 10<sup>6</sup> cells/plate) in 100 mm dishes (50-90% confluency) were transfected using Lipofectamine 2000 (Invitrogen). After 24 h, microsomal protein was prepared from the transfected cells. Following centrifugation, the cell pellet was resuspended in buffer (10 mM Tris-HCl, pH 7.4, 1 mM EDTA, 10% glycerol) followed by sonication and centrifugation (9,000 g, 20 min, 4 °C). The supernatant was additionally centrifuged (105,000 g, 1 h). The pellet was then dissolved in 100 to 200µl cold buffer (50 mM



Tris-HCl, pH 7.4, 1 mM EDTA, 150 mM KCl, 20% glycerol, and protease inhibitor cocktail).

#### *Western blot analyses*

Western blot analysis was also performed to determine the expression of CYP2C18 protein in liver and kidney microsomes from the transgenic mice along with Huh-7 and COS-7 cells transiently transfected with recombinant CYP2C18. Either 30  $\mu$ g of mouse liver microsomal protein, 40  $\mu$ g of mouse kidney microsomal protein or 25  $\mu$ g of microsomes from transfected cells were separated via SDS-PAGE on a 10% gel followed by wet-transfer to a nitrocellulose filter. The filters were blocked with 5% milk in TBS buffer and then incubated with the anti-CYP2C18 antibody diluted in TBS (1:500). This was followed by incubation with a 1:2000 dilution of a goat anti-rabbit secondary antibody conjugated to horseradish peroxidase (Dako Cytomation, Glostrup, Denmark) and detection using SuperSignal West Pico chemiluminescent substrate (Pierce, Rockford, IL).

To detect CYP2C19 in liver microsomes from transgenic mice the  $\alpha$ -hCYP2C antipeptide antiserum was used. Microsomes corresponding to 20  $\mu$ g protein were subjected to SDS-PAGE using a 10% gel. After transfer, the Hybond-C extra membrane (Amersham Pharmacia Biotech, Uppsala, Sweden) was blocked in TBS containing 0.05% (v/v) Tween 20 and 5% fat-free milk, and incubated with a 1:1000 dilution of the CYP2C antisera and further processed as described above.

*Statistical methods*

Genotype associated differences in *S*-mephenytoin and *R*-omeprazole metabolism within the male and female mouse groups were compared using the Mann-Whitney test.

## Results

### *Chromosomal integration*

Mice were made transgenic using a BAC clone fragment containing both the human *CYP2C18* and *CYP2C19* genes (Figure 1). Transgenic mice were identified by isolating gDNA from tail or ear tissue followed by transgene specific amplification using conventional PCR (Table 1). The primer specificity was evident due to the absence of any amplification product using gDNA from wt C57BL/6 mice (data not shown).

The chromosomal integration of the human clone was analysed using FISH. As evident from Figure 2, the genes were localized to region C1 of murine chromosome 2. The transgene copy number was determined using real time PCR and *CYP2C19* specific primers in combination with either murine *IL2* (*mIL2*) or human *IL2* (*hIL2*) as endogenous reference genes. The amplification plots for *CYP2C19*, *hIL2* and *mIL2* were linear throughout the tested concentration range (Figure 3) and the determined efficiencies were used in the subsequent relative copy number calculations. Comparison of four mouse gDNA samples with four human gDNA samples revealed the transgenic mouse genome to contain  $6.1 \pm 0.4$  times more copies of the *CYP2C19* gene compared to the reference human gDNA samples. Since the human genome contains two copies of the *CYP2C19* gene, the heterozygous mice would therefore contain  $12.1 \pm 0.9$  copies which would equate to an estimate of ~11-13 copies. Similar results were obtained in identical experiments using an alternative reference gene (*PCBP2*) instead of *IL2* (data not shown).

### *Expression at the mRNA level*

The expression of CYP2C18 and CYP2C19 mRNA was determined by real time PCR and isoform-specific primers. Total RNA was isolated from the liver, small intestine, kidney, heart, lung and brain from 26-31 week old male and female mice. As shown in Figure 4, there was a very abundant expression of CYP2C18 mRNA in liver of male mice with female expression levels approximately 10-fold less, a trend also observed in the kidney. Similarly, CYP2C19 mRNA was highly expressed in male livers and kidneys with much lower amounts observed in females. By contrast, no such sex difference was apparent in the small intestine, although this tissue expressed very high levels of both transcripts. Indeed, CYP2C19 mRNA expression was higher in the small intestine than in liver, and was also approximately 10-fold higher in small intestine than observed for CYP2C18 mRNA. Limited transcript expression was observed in both the lung and brain with no appreciable differences between transcripts or sex. Although transgene mRNA expression levels were the lowest in the heart, male mice expressed statistically significant greater amount of both transcripts in this tissue.

#### *Expression at the protein level*

Examination of the specificity of the CYP2C18 antiserum revealed that it did recognize recombinant CYP2C18 but not any CYP2C enzymes expressed in human liver microsomes (Figure 5A). Furthermore, specific CYP2C18 immunoreactive protein of the appropriate apparent molecular weight was observed in microsomes isolated from COS-7 cells transfected with CYP2C18 cDNA but not in similar experiments using Huh-7 cells (Figure 5B). Titration of recombinant CYP2C18 standards revealed a lower detection limit of 0.02 pmol (Figure 5B). However, immunoreactive protein could not be detected using liver microsomes from either transgenic or wt mice (Figure 5A) nor

in microsomal preparations from kidney (not shown). This result indicates that the level of CYP2C18 protein in the transgenic mice is either very low ( $<0.8$  pmol/mg) or nil.

The expression of CYP2C19 protein was examined using the  $\alpha$ -hCYP2C antipeptide antiserum directed towards the four C-terminal amino acids of CYP2C18, CYP2C19, CYP2C8, CYP2C9 and coincidentally CYP2C70 (the only murine CYP2C protein having this C-terminal sequence and thus this reactivity). As human CYP2C8 and CYP2C9 are not present in mice and CYP2C18 was undetectable using the CYP2C18 specific antibody, the  $\alpha$ -hCYP2C antiserum was used to quantitate CYP2C19 and CYP2C70 protein expression. As shown in Figure 6A, Western analysis of liver microsomal proteins from male mice using the  $\alpha$ -hCYP2C antiserum revealed a single immunoreactive protein band of the appropriate apparent molecular weight. Densitometric analyses revealed transgenic male mice to have 42% more immunoreactive protein than wt male mice (Figure 6B).

#### *Expression at the catalytic level*

Assessment of CYP2C dependent catalysis was done by examining the rate of hydroxylation of the CYP2C19 probes *S*-mephenytoin and *R*-omeprazole. In 9-week old male mice, a statistically significant increase ( $p<0.05$ ) in intrinsic clearance (as  $\mu\text{l/nmol P450/min}$ ) was observed in the transgenic CYP2C18/19 mice compared to their wt controls (Table 2). A much smaller and statistically insignificant increase in intrinsic clearance could be seen in transgenic female mice compared to wt controls, consistent with the limited expression of CYP2C19 mRNA. There was also a statistically significant reduction in the total microsomal cytochrome P450 content. Similar to the trend in intrinsic clearance, the difference was much greater and only

statically significant in male mice. These observations could suggest a concomitant down regulation of the endogenous murine P450 enzymes as a result of the transgene expression (Table 2).

Liver microsomes from transgenic and wt 12-week old males were incubated with *R*-omeprazole followed by quantitation of the 5'-hydroxylated metabolite. Linearity in the assay was assured with respect to protein and time. The results presented in Figure 7 demonstrate a statistically significant ( $p = 0.028$ ) 40% increase in the median rate of omeprazole hydroxylation in male transgenic mice compared to wt mice. This difference is similar in magnitude to the increase in CYP2C19 (and potentially CYP2C70) immunoreactive protein (Figure 6C).

## Discussion

Mice were made transgenic using a DNA fragment representing a contiguous 196 k bp region of the human genome containing the *CYP2C18* and *CYP2C19* genes and putative *cis*-acting regulatory regions. The transgene was found to have integrated into a single site composed of ~12 tandem copies in region C1 of mouse chromosome 2 (Figures 2 and 3). Obtaining such relatively high transgene copy numbers using BAC clones is not uncommon (Xing et al., 2007). Despite the high transgene copy number, Western blot analysis demonstrated only an approximate 40% increase in protein immunoreactive with a CYP2C19 and CYP2C70 targeted antibody in transgenic male mice as compared to wt controls (Figure 6). This relationship was also reflected in similar increases in rates of liver microsomal *S*-mephenytoin and *R*-omeprazole hydroxylation. Interestingly, there was also a reduction in total hepatic cytochrome P450 content in the transgenic mice compared to wt. Mirroring the trend observed in mRNA expression, the difference was much greater in male mice. One possible explanation for the higher levels of CYP2C19 mRNA observed in the liver of the transgenic mice with only a modest increase in hepatic CYP2C immunoreactive protein could be that murine P450 enzymes are down regulated in a feedback regulatory mechanism as a result of the expression of the *CYP2C19* transgene. As CYPs have a critical role in regulating the levels of many endogenous endocrine factors, it could be suggested that the expression of the transgenic human CYP2C19 enzyme could play a compensatory role.

Interestingly, real time PCR analysis revealed that both the *CYP2C18* and *CYP2C19* genes were expressed in a sexually dimorphic manner in the liver, kidney and heart but not in the small intestine, lung or brain (Figure 4). Although male mice expressed

similar amounts of both CYP2C18 and CYP2C19 transcripts in liver, females expressed levels which were only about 1/10 to 1/100 of this level, respectively. A different relationship was observed in the kidneys, with females expressing roughly similar amounts of both human CYP2C transcripts, and males expressing 20- and 5-fold greater amounts of CYP2C18 and CYP2C19 mRNA, respectively. These results clearly indicate the human genes are subject to murine and tissue specific regulatory factors.

Important sex differences are evident in the expression of specific *CYP2C* genes in rats. Sex difference in growth hormone (GH) secretory patterns result in differing levels of transcriptional activation, with transcriptional factors such STAT5 playing a critical role (Park and Waxman, 2001). By contrast, no such sexually dimorphic CYP2C isoform expression is seen in human livers. Interestingly, our data from the transgenic mice indeed suggest that the factors controlling the sexually dimorphic expression of rodent *CYP2C* genes can interact with the regulatory elements of the *CYP2C18* and *CYP2C19* genes resulting in sexually dimorphic expression analogous to the male-specific *CYP2C11* gene in the rat (Waxman and O'Connor, 2006; Thangavel and Shapiro, 2007) and the *CYP2D* genes in mouse liver (Sueyoshi et al., 1999). Thus, sexually dimorphic *CYP* gene expression in rodents, as opposed to humans, is not necessarily dependent on gene structure *per se* but rather the presence of sex- and tissue-specific factors for transcriptional regulation of *CYP2C* gene expression. Our findings and model system would therefore be of great value in the future identification of the regulatory elements responsible for sexually dimorphic gene expression. Interestingly, Cheung et al. observed sexually dimorphic hepatic expression of CYP3A4 in transgenic mice; however, female mice were found to express significant amounts of CYP3A4 mRNA and protein whereas neither CYP3A4 mRNA nor protein



could be detected in adult males (Cheung et al., 2006). Furthermore, by administering a constant GH infusion via a subcutaneous minipump to override the normally pulsatile male plasma GH profile, they were able to clearly demonstrate a feminization of the expression of *CYP3A4* and of the endogenous murine *Cyp2b* and *Cyp3a44* genes, in male mice. It is plausible that GH could have a similar role in the tissue- and sex-preferential expression of CYP2C18 and CYP2C19 observed in the present study.

CYP2C19 mRNA was most abundant in the intestine and liver followed by kidney with only moderate amounts being observed in lung and brain. The high level of intestinal and hepatic CYP2C19 mRNA expression is consistent with previous studies in humans demonstrating similar levels of both CYP2C19 associated metabolic activity and mRNA expression in the liver and intestine (Lapple et al., 2003; Galetin and Houston, 2006; Bieche et al., 2007).

The relationship of mRNA levels correlating with levels of immunoreactive protein and catalytic activity determinations, held true in studies of 12-week old transgenic male mice which demonstrated a 42% increase in immunodetectable hepatic CYP2C19 and/or CYP2C70 compared to wt mice. A concomitant increase in the rate of hepatic *R*-omeprazole 5'-hydroxylation was seen (Figure 7). In liver microsomes from 9-week old transgenic males, *S*-mephenytoin intrinsic clearance was significantly increased, on the order of 3-fold greater than wt controls (Table 2). Taken together, these data indicate that the human CYP2C19 mRNA expressed in the male mice is indeed translated into functionally active CYP2C19 enzyme, although at a much lower level than expected from the high gene copy number (see above). By contrast, the absence of a statistically significant increase in *S*-mephenytoin hydroxylation in liver microsomes

from female mice was in accordance with the observed very low levels of CYP2C19 mRNA (Figure 4).

While the above results demonstrate that the transgenic *CYP2C19* gene was translated into functional protein, this clearly was not the case for *CYP2C18*, as evident using CYP2C18 specific antibodies. Indeed the CYP2C18 protein has not been found in detectable amounts in any human tissues (Goldstein, 2001) in spite of high levels of CYP2C18 mRNA (Nishimura et al., 2003). The consistency of the events following transcription of the *CYP2C18* gene along with the apparent insensitivity to any of the alterations associated with heterologous expression, as demonstrated by the absence of CYP2C18 in the transgenic mice, was somewhat unexpected and the underlying reasons remain unknown. Transient transfection studies were performed using cell lines derived from different tissue types to both further validate the CYP2C18 targeted antibody as well as to investigate any potential relationship between the translation or stability of CYP2C18 protein and any cell-type specific regulatory factors. It was shown that the CYP2C18 cDNA was effectively translated into detectable protein in the kidney cell derived COS-7 cell line whereas the efficiency was much less in the in Huh-7 hepatoma cell line (Figure 5). Despite these observations, CYP2C18 protein was not detected in kidney microsomes prepared from transgenic mice. It is conceivable these tissues contain factors, such as regulatory RNAs, which prevent translation of the CYP2C18 mRNA. It might also be possible that the enzyme is not properly folded due to the absence of required chaperone proteins and thus subject to proteolytic degradation. Further experiments might shed light on this phenomenon and help to identify the necessary components required for CYP2C18 translation and folding. Nevertheless, the results obtained here indicate that the alterations in CYP2C protein

and catalytic activity levels observed in the transgenic mice are due solely to the expression of a functional CYP2C19 enzyme and not CYP2C18.

In conclusion, our results show that the transgenic mice express CYP2C18 and CYP2C19 mRNAs at relatively high levels in liver, kidney and small intestine and that both genes are subject to sexually dimorphic regulation in the liver, kidney and heart. Future studies will attempt to identify the sex- and tissue-specific factors responsible for the transcriptional regulation of *CYP2C* gene expression. The significantly increased hydroxylation of *S*-mephenytoin and *R*-omeprazole hydroxylation observed in transgenic male mice suggests that this male mouse model has a more human-like metabolism of CYP2C19 substrates than wt C57BL/6 mice. This model could be potentially useful in early drug discovery and development, as a tool for pharmacological and toxicological studies of drug candidates that are specific substrates for human CYP2C19.

## **Acknowledgements**

We would like to thank Charlotta Ungmann and Golpar Pirzadeh for their help with preliminary animal characterization. We are indebted to Dr Robert Edwards and Dr Eric Johnson for their generous gifts of CYP2C antibodies. We also wish to acknowledge Tommy B. Andersson, Kjell Andersson and Lars Weidolf from AstraZeneca for their assistance, expertise and for graciously providing analytical standards.

## References

- Bieche I, Narjoz C, Asselah T, Vacher S, Marcellin P, Lidereau R, Beaune P and de Waziers I (2007) Reverse transcriptase-PCR quantification of mRNA levels from cytochrome (CYP)1, CYP2 and CYP3 families in 22 different human tissues. *Pharmacogenet Genomics* **17**:731-742.
- Bogaards JJ, Bertrand M, Jackson P, Oudshoorn MJ, Weaver RJ, van Bladeren PJ and Walther B (2000) Determining the best animal model for human cytochrome P450 activities: a comparison of mouse, rat, rabbit, dog, micropig, monkey and man. *Xenobiotica* **30**:1131-1152.
- Chen Y, Ferguson SS, Negishi M and Goldstein JA (2003) Identification of constitutive androstane receptor and glucocorticoid receptor binding sites in the CYP2C19 promoter. *Mol Pharmacol* **64**:316-324.
- Cheung C, Yu AM, Chen CS, Krausz KW, Byrd LG, Feigenbaum L, Edwards RJ, Waxman DJ and Gonzalez FJ (2006) Growth hormone determines sexual dimorphism of hepatic cytochrome P450 3A4 expression in transgenic mice. *J Pharmacol Exp Ther* **316**:1328-1334.
- De Preter K, Speleman F, Combaret V, Lunec J, Laureys G, Eussen BH, Francotte N, Board J, Pearson AD, De Paepe A, Van Roy N and Vandesompele J (2002) Quantification of MYCN, DDX1, and NAG gene copy number in neuroblastoma using a real-time quantitative PCR assay. *Mod Pathol* **15**:159-166.
- Edwards RJ, Adams DA, Watts PS, Davies DS and Boobis AR (1998) Development of a comprehensive panel of antibodies against the major xenobiotic metabolising forms of cytochrome P450 in humans. *Biochem Pharmacol* **56**:377-387.

- Furuta T, Ohashi K, Kamata T, Takashima M, Kosuge K, Kawasaki T, Hanai H, Kubota T, Ishizaki T and Kaneko E (1998) Effect of genetic differences in omeprazole metabolism on cure rates for *Helicobacter pylori* infection and peptic ulcer. *Ann Intern Med* **129**:1027-1030.
- Galetin A and Houston JB (2006) Intestinal and hepatic metabolic activity of five cytochrome P450 enzymes: impact on prediction of first-pass metabolism. *J Pharmacol Exp Ther* **318**:1220-1229.
- Gerbal-Chaloin S, Pascussi JM, Pichard-Garcia L, Daujat M, Waechter F, Fabre JM, Carrere N and Maurel P (2001) Induction of CYP2C genes in human hepatocytes in primary culture. *Drug Metab Dispos* **29**:242-251.
- Goldstein JA (2001) Clinical relevance of genetic polymorphisms in the human CYP2C subfamily. *Br J Clin Pharmacol* **52**:349-355.
- Hellemans J, Mortier G, De Paepe A, Speleman F and Vandesompele J (2007) qBase relative quantification framework and software for management and automated analysis of real-time quantitative PCR data. *Genome Biol* **8**:R19.
- Hillig T, Krstrup P, Fleming I, Osada T, Saltin B and Hellsten Y (2003) Cytochrome P450 2C9 plays an important role in the regulation of exercise-induced skeletal muscle blood flow and oxygen uptake in humans. *J Physiol* **546**:307-314.
- Hoebbeck J, Speleman F and Vandesompele J (2007) Real-time quantitative PCR as an alternative to Southern blot or fluorescence in situ hybridization for detection of gene copy number changes. *Methods Mol Biol* **353**:205-226.
- Ingelman-Sundberg M, Sim SC, Gomez A and Rodriguez-Antona C (2007) Influence of cytochrome P450 polymorphisms on drug therapies: Pharmacogenetic, pharmacoepigenetic and clinical aspects. *Pharmacol Ther* **116**:496-526.

- Klose TS, Blaisdell JA and Goldstein JA (1999) Gene structure of CYP2C8 and extrahepatic distribution of the human CYP2Cs. *J Biochem Mol Toxicol* **13**:289-295.
- Klotz U (2006) Clinical impact of CYP2C19 polymorphism on the action of proton pump inhibitors: a review of a special problem. *Int J Clin Pharmacol Ther* **44**:297-302.
- Lapple F, von Richter O, Fromm MF, Richter T, Thon KP, Wisser H, Griese EU, Eichelbaum M and Kivisto KT (2003) Differential expression and function of CYP2C isoforms in human intestine and liver. *Pharmacogenetics* **13**:565-575.
- Lindqvist A, Hilke S and Skoglund E (2004) Generic three-column parallel LC-MS/MS system for high-throughput in vitro screens. *J Chromatogr A* **1058**:121-126.
- Lofgren S, Hagbjork AL, Ekman S, Fransson-Steen R and Terelius Y (2004) Metabolism of human cytochrome P450 marker substrates in mouse: a strain and gender comparison. *Xenobiotica* **34**:811-834.
- Lowry OH, Rosebrough NJ, Farr AL and Randall RJ (1951) Protein measurement with the Folin phenol reagent. *J Biol Chem* **193**:265-275.
- Maines MD (1999) *Current protocols in toxicology*. John Wiley, New York.
- Meier UT, Dayer P, Male PJ, Kronbach T and Meyer UA (1985) Mephenytoin hydroxylation polymorphism: characterization of the enzymatic deficiency in liver microsomes of poor metabolizers phenotyped in vivo. *Clin Pharmacol Ther* **38**:488-494.
- Nebert DW and Russell DW (2002) Clinical importance of the cytochromes P450. *Lancet* **360**:1155-1162.
- Niioka T, Uno T, Sugimoto K, Sugawara K, Hayakari M and Tateishi T (2007) Estimation of CYP2C19 activity by the omeprazole hydroxylation index at a

single point in time after intravenous and oral administration. *Eur J Clin Pharmacol* **63**:1031-1038.

Nishimura M, Yaguti H, Yoshitsugu H, Naito S and Satoh T (2003) Tissue distribution of mRNA expression of human cytochrome P450 isoforms assessed by high-sensitivity real-time reverse transcription PCR. *Yakugaku Zasshi* **123**:369-375.

Omura T and Sato R (1964) The Carbon Monoxide-Binding Pigment of Liver Microsomes. I. Evidence for Its Hemoprotein Nature. *J Biol Chem* **239**:2370-2378.

Park SH and Waxman DJ (2001) Inhibitory cross-talk between STAT5b and liver nuclear factor HNF3beta: impact on the regulation of growth hormone pulse-stimulated, male-specific liver cytochrome P-450 gene expression. *J Biol Chem* **276**:43031-43039.

Pascussi JM, Gerbal-Chaloin S, Drocourt L, Maurel P and Vilarem MJ (2003) The expression of CYP2B6, CYP2C9 and CYP3A4 genes: a tangle of networks of nuclear and steroid receptors. *Biochim Biophys Acta* **1619**:243-253.

Richardson TH, Griffin KJ, Jung F, Raucy JL and Johnson EF (1997) Targeted anti-peptide antibodies to cytochrome P450 2C18 based on epitope mapping of an inhibitory monoclonal antibody to P450 2C51. *Arch Biochem Biophys* **338**:157-164.

Sambrook J and Russell DW (2001) *Molecular cloning : a laboratory manual*. Cold Spring Harbor Laboratory Press, Cold Spring Harbor, N.Y.

Sueyoshi T, Yokomori N, Korach KS and Negishi M (1999) Developmental action of estrogen receptor-alpha feminizes the growth hormone-Stat5b pathway and expression of Cyp2a4 and Cyp2d9 genes in mouse liver. *Mol Pharmacol* **56**:473-477.



- Thangavel C and Shapiro BH (2007) A molecular basis for the sexually dimorphic response to growth hormone. *Endocrinology* **148**:2894-2903.
- Tybring G, Bottiger Y, Widen J and Bertilsson L (1997) Enantioselective hydroxylation of omeprazole catalyzed by CYP2C19 in Swedish white subjects. *Clin Pharmacol Ther* **62**:129-137.
- Vandesompele J, De Preter K, Pattyn F, Poppe B, Van Roy N, De Paepe A and Speleman F (2002) Accurate normalization of real-time quantitative RT-PCR data by geometric averaging of multiple internal control genes. *Genome Biol* **3**:RESEARCH0034.
- Walsky RL and Obach RS (2004) Validated assays for human cytochrome P450 activities. *Drug Metab Dispos* **32**:647-660.
- Waxman DJ and O'Connor C (2006) Growth hormone regulation of sex-dependent liver gene expression. *Mol Endocrinol* **20**:2613-2629.
- Xing L, Salas M, Lin CS, Zigman W, Silverman W, Subramaniam S, Murty VV and Tycko B (2007) Faithful tissue-specific expression of the human chromosome 21-linked COL6A1 gene in BAC-transgenic mice. *Mamm Genome* **18**:113-122.

## Footnotes

This research was in part supported by a grant from The Swedish Research council.

\*These authors contributed equally to this work.

### *Present Addresses*

Medivir AB, P.O. Box 1086, SE-141 22 Huddinge, Sweden: AL, YT

Dept. of Clinical Pharmacotherapeutics, Tohoku Pharmaceutical University,

4-4-1 Komatsushima Aoba-ku, Sendai 981-8558 Japan: MH

## Legends to figures

**Figure 1.** Schematic representation of bacterial artificial chromosome (BAC) RP11-466J14, used to generate the CYP2C18/19 transgenic mice. The 5' end of the BAC is located 5,828 base pairs upstream of exon 1 of *CYP2C18*. The 3' end is located 30,869 base pairs downstream of exon 9 of *CYP2C19*. The arrows indicate the gene orientations

**Figure 2.** FISH analysis to determine the chromosomal location of the CYP2C18/19 transgene. A single hybridization signal is observed at region C1 of mouse chromosome 2. Nick translated DNA fragments from the ~196k bp DNA insert from BAC clone RP11-466J14 were used as hybridization probes. Chromosomal preparations from A) heterozygous mouse, and B) homozygous mouse. C1) Reference DAPI banding pattern of mouse chromosome 2 C2) DAPI banding pattern prior to probe hybridization C3) superimposed probe hybridization signal (red).

**Figure 3.** *CYP2C19* gene copy number determination in transgenic mice. Standard curves obtained from amplifying either *CYP2C19* (2C19), murine *IL2* (mIL2) or human *IL2* (hIL2) from serial two-fold dilutions of either mouse or human genomic DNA (2 to 0.25 ng). Data are plotted as cycle threshold versus log picogram DNA.

**Figure 4.** CYP2C18 (A) and CYP2C19 (B) mRNA expression in transgenic male (●) and female (○) mice 26-31 weeks of age using reverse transcribed total RNA from liver, small intestine (S. Intestine), kidney, heart, lung and brain. Relative expression levels of each gene transcript were determined using real time PCR and gene specific primers (Table 1). The geometric mean of two reference transcripts (GAPDH and

HPRT) was used to normalize the expression levels of CYP2C18 and CYP2C19. Bars denote mean values. Male and female mice were compared using the Mann-Whitney test.

**Figure 5.** Western blot analysis of CYP2C18 expression using a CYP2C18 specific antibody.

**A.** Expression of CYP2C18 in liver microsomes (30 $\mu$ g) from transgenic and wildtype mice. wt: wildtype, r2C18: recombinant CYP2C18 Supersomes<sup>TM</sup>, HLM: human liver microsomes

**B.** Expression of CYP2C18 in Huh-7 cells and in COS-7 cells (25 $\mu$ g) after transfection with CYP2C18 cDNA. Amounts of recombinant CYP2C18 standards (Supersomes<sup>TM</sup>) used to approximate lowest detectable amount of CYP2C18 protein. (+): transfected with CYP2C18 cDNA, (-): transfected with empty vector.

**Figure 6.** Western blot analysis of CYP2C19 and CYP2C70 protein expression in liver microsomes (20  $\mu$ g) from transgenic and wildtype mice using the  $\alpha$ -hCYP2C antipeptide antibody targeted against the four C-terminal amino acids of the four human CYP2Cs and murine CYP2C70 (representative blots shown). Tg: Heterozygous transgenic, wt: wildtype

**A.** CYP2C19 and CYP2C70 expression levels in 12-week old male transgenic and male wildtype mice.

**B.** Densitometric analyses reveals a 42% increase in CYP2C19 and/or CYP2C70 immunoreactive protein in liver microsomes from 12-week old male transgenic (n=4) compared to wildtype (n=9) mice.  $p = 0.034$  (Mann-Whitney test).

**Figure 7.** *R*-omeprazole 5'-hydroxylation in liver microsomes from 12-week old male transgenic (n=4) and male wildtype mice (n=10). Mean values  $\pm$  SEM. \*:  $p < 0.028$  (Mann-Whitney test). wt: wildtype, Tg = heterozygous transgenic

**Table 1.** Primers sequences

	Target	Strand	Primer sequence (5'-3')
2C18 Intron 6	gDNA / Genotyping	Sense	GGCAAGAAACACTTCATGAGCACT
		Antisense	ATTCAGTTAAGGCCTCCCTTTTCC
2C19 Intron 5	gDNA / Genotyping	Sense	CAAGATGGGCCTTATAAAGTTGGC
		Antisense	GAAGAAATTGGAACCCTCATGTCC
CYP2C19	gDNA / Copy Number	Sense	GCCATTCCCCTGGCTGAAAG
		Antisense	ACGAACTAGGAGGGAGATCC
Human IL2	gDNA / Copy Number	Sense	TGCACATAATCTCATCTTTCTAACACTCTT
		Antisense	TTGAAAGCGCAATAGATGGACAT
Mouse IL2	gDNA / Copy Number	Sense	GCTCCACACTGAATACCCAAGAC
		Antisense	GAAGAGGTTTGACAAGATAACACGTAGT
CYP2C18	mRNA	Sense	CTCATCCCCAAGGGCAGC
		Antisense	GGTTGGGGAATTCTTTGTCATTG
CYP2C19*	mRNA	Sense	GAAAAATTGAATGAAAACATCAGGATTG
		Antisense	CGAGGGTTGTTGATGTCCATC
GAPDH**	mRNA	Sense	TGGCAAAGTGGAGATTGTTGCC
		Antisense	AAGATGGTGATGGGCTTCCCG
HPRT***	mRNA	Sense	GTCAACGGGGGACATAAAAAG
		Antisense	TGGGGCTGTACTGCTAACC

\* Taken from Klose et al. (Klose et al. 1999) with minor modification

\*\* Taken from Mills et al. (Mills et al. 2001)

\*\*\* Taken from Hoffman (Hofmann et al. 2000)

<Table 2. Apparent enzyme kinetic parameters for S-mephenytoin metabolism in liver microsomes from 9-week old wt and heterozygous CYP2C18/19 transgenic mice.

		Males			Females		
		wt (n=6) <sup>1</sup>	Het (n=8)	p-value	wt (n=6)	Het (n=8) <sup>2</sup>	p-value
V <sub>max</sub> (pmol / nmol P450 / min)	Mean ± SD	41.9 ± 11.0	68.8 ± 56.2		49.4 ± 10.5	40.6 ± 5.3	
	Median (range)	40.1 (29.5-58.5)	47.0 (31.9-201.6)	0.435	44.7 (40.9-66.9)	39.9 (33.9-47.3)	0.240
K <sub>m</sub> (μM)	Mean ± SD	56.5 ± 24.4	53.9 ± 58.7		77.1 ± 19.3	54.8 ± 33.5	
	Median (range)	52.1 (32.3-102.6)	28.6 (8.1-174.9)	0.181	70.7 (54.9-101.7)	50.0 (10.0-112.9)	0.181
CL <sub>int</sub> <sup>3</sup> (μl / nmol P450 / min)	Mean ± SD	0.77 ± 0.25	2.50 ± 3.04		0.66 ± 0.14	1.51 ± 1.54	
	Median (range)	0.71 (0.52-1.11)	1.40 (0.62-9.77)	<b>0.030</b>	0.65 (0.44-0.85)	0.96 (0.44-4.57)	0.180
P450 content (nmol P450 / mg mic prot)	Mean ± SD	0.56 ± 0.16	0.35 ± 0.08		0.50 ± 0.09	0.39 ± 0.09	
	Median (range)	0.60 (0.37-0.76)	0.33 (0.25-0.53)	<b>0.011</b>	0.51 (0.39-0.63)	0.41 (0.26-0.48)	0.065
Liver weight (g)	Mean ± SD	1.40 ± 0.17	1.24 ± 0.24		0.98 ± 0.04	0.93 ± 0.08	
	Median (range)	1.43 (1.08-1.54)	1.21 (1.01-1.74)	0.108	0.98 (0.91-1.03)	0.95 (0.83-1.02)	0.491
mg mic prot / g liver	Mean ± SD	21.1 ± 8.21	25.0 ± 3.6		22.9 ± 3.4	24.0 ± 5.5	
	Median (range)	21.2 (8.3-33.9)	25.4 (17.6-28.7)	0.181	23.2 (18.7-27.9)	24.1 (15.7-34.6)	0.662
nmol P450 / g liver	Mean ± SD	12.9 ± 3.4	8.6 ± 1.7		11.4 ± 2.4	9.9 ± 1.9	0.254
	Median (range)	12.7 (8.1-17.7)	8.3 (7.2-12.3)	<b>0.019</b>	11.7 (7.6-14.3)	10.1 (7.2-11.8)	0.180

The table shows parametric and non-parametric parameters for each group. Statistical analyses were done using the Mann-Whitney test.

1. For the parameters V<sub>max</sub>, CL<sub>int</sub>, P450 content and nmol P450/g liver; n=5
2. For the parameters V<sub>max</sub>, CL<sub>int</sub>, P450 content and nmol P450/g liver; n=6
3. CL<sub>int</sub> calculated as V<sub>max</sub>/K<sub>m</sub>

wt: wildtype C56BL/6 mice, Het: heterozygous CYP2C18/19 transgenic mice, mic

prot: microsomal protein

Figure 1

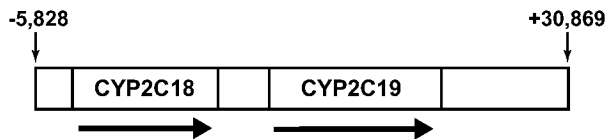




Figure 2

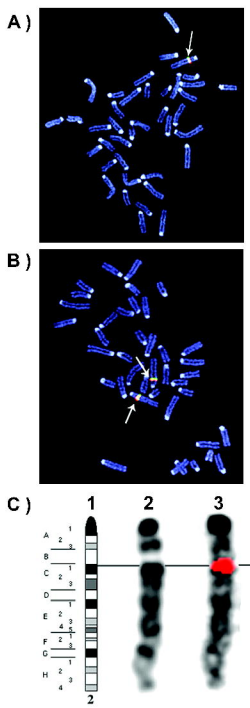


Figure 3

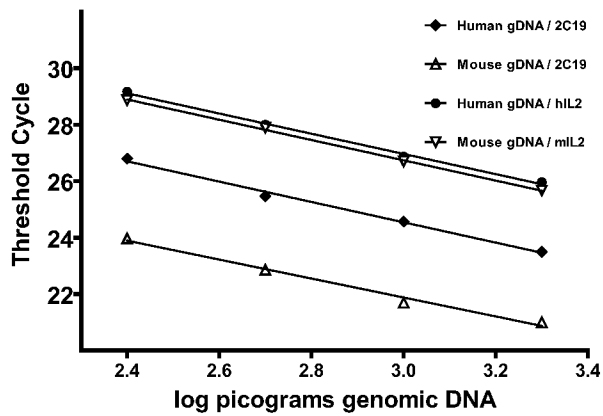


Figure 4

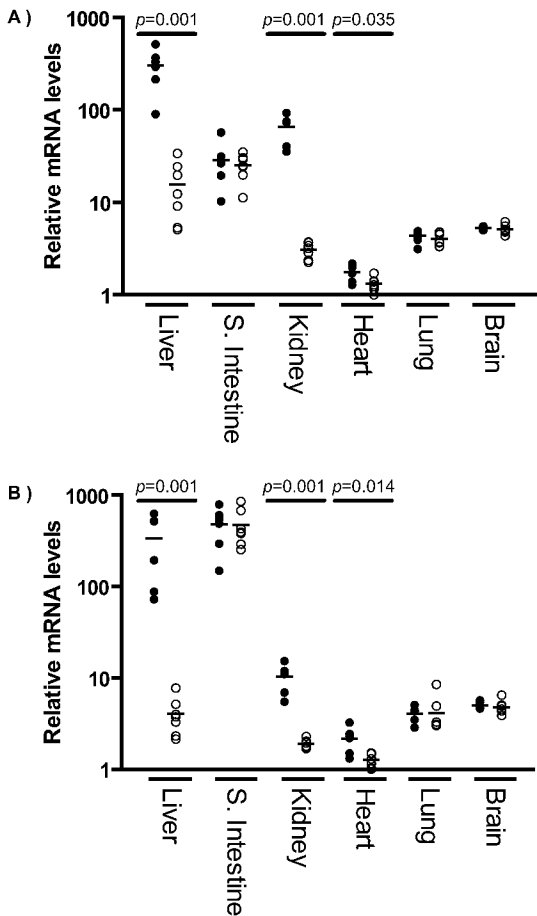


Figure 5

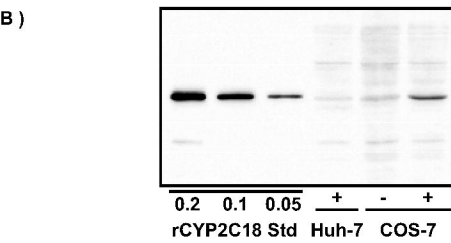
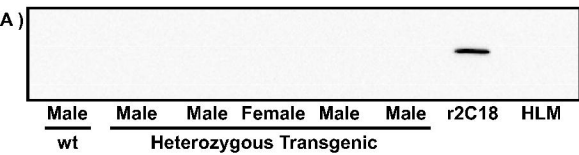
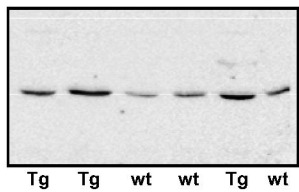


Figure 6

A)



B)

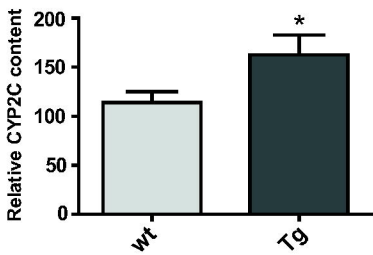


Figure 7

